Journal of Sound and Vibration (2002) **252**(2), 223–238
doi:10.1006/jsvi.2001.3749, available online at http://www.idealibrary.com on IDEAL®

IMPROVED DAMAGE IDENTIFICATION METHOD BASED ON MODAL INFORMATION

J.-T. KIM

Department of Ocean Engineering, Pukyong National University, Nam-gu, Pusan 608-737, *Korea.*
E-mail: idis@pknu.ac.kr

AND

N. STUBBS

Department of Civil Engineering, Texas A&M University, College Station, TX 77843, *U.S.A.*

(*Received* 17 *July* 2000, *and in final form* 2 *April* 2001)

In this paper, a newly derived algorithm to predict locations and severities of damage in structures using changes in modal characteristics is presented. First, two existing algorithms of damage detection are reviewed and the new algorithm is formulated in order to improve the accuracy of damage localization and severity estimation by eliminating erratic assumptions and limits in the existing algorithms. Next, the damage prediction accuracy is numerically assessed for each algorithm when applied to a two-span continuous beam for which pre- and post-damage modal parameters are available for only a few modes of vibration. Compared to the existing damage detection algorithms, the new algorithm improved the accuracy of damage localization and severity estimation results in the test beam.

1. INTRODUCTION

This paper deals with the general problem of utilizing changes in dynamic modal parameters of structures to non-destructively detect, locate, and estimate the severity of damage in these structures. Structural damage may be defined as any deviation of a geometric or material property defining a structure that may result in unwanted responses of the structure. A solution to this problem is important for at least two reasons. Firstly, damage localization and severity estimation are the first two steps in the broader category of damage assessment. Secondly, a timely damage assessment could produce desirable consequences such as saving of lives, reduction of human suffering, protection of property, increased reliability, increased productivity of operations, and reduction in maintenance costs.

During the past decade, a significant amount of research has been conducted in the area of damage detection using the dynamic response of a structure. Research efforts have been made to detect structural damage directly from dynamic response measurements in the time domain, e.g., the random decrement technique [1, 2], or from frequency response functions (FRF) [3]. Also, methods have been proposed to detect damage using system identification techniques [4, 5]. Many research studies have been conducted in the area of non-destructive damage detection (NDD) using changes in modal parameters. Research studies have related changes in natural frequencies to changes in beam properties such as cracks, notches or

0022-460X/02/$35.00

other geometrical changes [6–8]. Studies have also focused on the possibility of using the vibration characteristics of structures as an indication of structural damage [9–12]. Since 1988, studies on the topic appear to be accelerating. Attempts have been made to monitor structural integrity of bridges [3, 13], to investigate feasibility of damage detection in large-space structures using changes in modal parameters [14, 15], and to localize damage in beam-type structures using changes in mode shapes characteristics [16, 17].

Despite these research efforts, however, many problems related to vibration-based damage detection remain unsolved today. Outstanding needs remain to locate and estimate the severity of damage: (a) in structures with only few available modes, (b) in structures with many members, (c) in structures for which baseline modal responses are not available, and (d) in an environment of uncertainty associated with modelling, measurement, and processing errors.

In this paper, we present a new vibration-based NDD algorithm to locate and estimate severity of damage in structures. The proposed methodology is presented here in two parts. In the first part, we outline vibration-based NDD algorithms. We first review existing NDD algorithms proposed by Kim and Stubbs [16, 18]. Then we formulate a new NDD algorithm to improve its accuracy in damage localization and severity estimation by eliminating erratic assumptions and limits in the existing NDD algorithms. In the second part, we demonstrate the feasibility of the new NDD algorithm using numerical examples. The new NDD algorithm and two existing ones are evaluated by predicting damage locations and estimating severities of damage in a two-span continuous beam for which limited modal parameters are available for a few modes of vibration. The performance of each algorithm is assessed quantifying the accuracy of damage prediction results.

In the structures of interest in this study, the objective is to detect low magnitude damage at a very early stage. In such cases, changes in modal parameters between the undamaged and damaged structures are small and the application of the modal assurance criterion provides a reliable means of identifying the modes [19]. In the extreme case when only the damaging mode is available the technique of generating a baseline modal model using the updating of a finite element model of the structure can be used [18].

2. EXISTING DAMAGE DETECTION ALGORITHMS

For a linear, undamaged, skeletal structure with ne elements and n nodes, the ith modal stiffness of the arbitrary structure is given by

$$K_i = \Phi_i^{\mathrm{T}} \mathbf{C} \Phi_i, \tag{1}$$

where Φ_i is the ith modal vector and $\mathbf{C}$ is the system stiffness matrix. The contribution of jth member to ith modal stiffness, K_{ij}, is given by

$$K_{ij} = \Phi_i^{\mathrm{T}} \mathbf{C}_j \Phi_i, \tag{2}$$

where $\mathbf{C}_j$ is the contribution of jth member to the system stiffness matrix. Then, the fraction of modal energy (i.e., the undamaged modal sensitivity) of the ith mode and the jth member is defined as

$$F_{ij} = K_{ij}/K_i. \tag{3}$$

Let the corresponding modal parameters in equations (1)–(3) associated with a subsequently damaged structure be characterized by asterisks. Then for the damaged

structure, the damaged sensitivity of the ith mode and the jth member is defined as

$$F_{ij}^* = K_{ij}^*/K_i^*, \tag{4}$$

in which the quantities K_{ij}^* and K_i^* are given by

$$K_{ij}^* = \Phi_i^{*\mathrm{T}} \mathbf{C}_j^* \Phi_i^*, \qquad K_i^* = \Phi_i^{*\mathrm{T}} \mathbf{C}^* \Phi_i^*. \tag{5a, b}$$

The quantities $\mathbf{C}_j$ and $\mathbf{C}_j^*$ in equations (2) and (5a) may be written as follows:

$$\mathbf{C}_j = E_j \mathbf{C}_{j0}, \qquad \mathbf{C}_j^* = E_j^* \mathbf{C}_{j0}, \tag{6a, b}$$

where the scalars E_j and E_j^* are parameters representing material stiffness properties of undamaged and damaged jth members, respectively. The matrix $\mathbf{C}_{j0}$ involves only geometric quantities (and possibly terms containing Poisson's ratio) and it can represent beam or plate elements.

2.1. DAMAGE INDEX A [16]

Suppose we make an approximation that the modal sensitivities for the ith mode and the jth location is the same for both undamaged and damaged structure (i.e., $F_{ij}^* \approx F_{ij}$). Then equations (3) and (4) are combined and reduced to the following expression:

$$F_{ij}^*/F_{ij} = (K_{ij}^* K_i)/(K_{ij} K_i^*) = 1. \tag{7}$$

On substituting equations (1), (2), (5), and (6) into equation (7) and by rearranging, a damage index β_j of jth member (and for nm modes involved) is obtained by [16]

$$\beta_j = \frac{E_j}{E_j^*} = \frac{\sum_{i=1}^{nm} \gamma_{ij}^* K_i}{\sum_{i=1}^{nm} \gamma_{ij} K_i^*}, \tag{8}$$

in which $\gamma_{ij} = \Phi_i^{\mathrm{T}} \mathbf{C}_{j0} \Phi_i$ and $\gamma_{ij}^* = \Phi_i^{*\mathrm{T}} \mathbf{C}_{j0} \Phi_i^*$ and damage is indicated at jth member if $\beta_j > 1$.

The severity of damage in the jth member is estimated as follows. Let the fractional change in the stiffness of the jth member be given by the severity estimator, α_j, then

$$E_j^* = E_j \left(1 + \frac{\mathrm{d}E_j}{E_j}\right) = E_j(1 + \alpha_j). \tag{9}$$

Combining equations (8) and (9) yields

$$\alpha_j = \frac{\sum_{i=1}^{nm} \gamma_{ij} K_i^*}{\sum_{i=1}^{nm} \gamma_{ij}^* K_i} - 1, \quad \alpha_j \geqslant -1, \tag{10}$$

where damage severity is indicated as the reduction in stiffness in the jth member if $\alpha_j < 0$.

2.2. DAMAGE INDEX B [17]

From equation (8), damage is indicated at jth member if $\beta_j > 1$. However, the same equation becomes singular if the denominator goes zero. This condition will occur when

simultaneously, the element size approaches zero and the element location coincides with a nodal point of a mode. To overcome this limitation (i.e., the division by zero difficulty), an approximation is made such that the axis of reference for the modal sensitivities is shifted by a value of 1·0 (i.e., $F_{ij} \to F_{ij} + 1$ and $F^*_{ij} \to F^*_{ij} + 1$). Adding unity to both the numerator and the denominator of equation (7) yields

$$(F^*_{ij} + 1)/(F_{ij} + 1) = [(K^*_{ij} + K^*_i)K_i]/[(K_{ij} + K_i)K^*_i] = 1. \tag{11}$$

On substituting equations (1), (2), (5), and (6) into equation (11) and by rearranging, a damage index β_j of jth member (and for nm modes) is obtained by

$$\beta_j = \frac{E_j}{E^*_j} = \frac{\sum_{i=1}^{nm} (\gamma^*_{ij} + \sum_{k=1}^{ne} \gamma^*_{ik})K_i}{\sum_{i=1}^{nm} (\gamma_{ij} + \sum_{k=1}^{ne} \gamma_{ik})K^*_i}, \tag{12}$$

where damage is indicated at the jth location if $\beta_j > 1$. Once damage is localized at the jth member, its severity can be estimated in the same way as described previously. Applying equation (12) to equation (9) yields

$$\alpha_j = \frac{\sum_{i=1}^{nm} (\gamma_{ij} + \sum_{k=1}^{ne} \gamma_{ik})K^*_i}{\sum_{i=1}^{nm} (\gamma^*_{ij} + \sum_{k=1}^{ne} \gamma^*_{ik})K_i} - 1, \quad \alpha_j \geqslant -1, \tag{13}$$

where damage severity is indicated as the reduction in stiffness in the jth member if $\alpha_j < 0$.

3. UPDATED ALGORITHM—DAMAGE INDEX C

Let λ_i and λ^*_i be the ith eigenvalues of pre- and post-damage multi-degree-of-freedom (mdof) structural systems respectively. Then the ith eigenvalues can be related to the following forms:

$$\lambda^*_i = \lambda_i + \mathrm{d}\lambda_i = (K_i + \mathrm{d}K_i)/(M_i + \mathrm{d}M_i), \tag{14}$$

in which K_i and M_i are the ith modal stiffness and the ith modal mass of the undamaged system respectively. Also, $\mathrm{d}\lambda_i$, $\mathrm{d}K_i$, and $\mathrm{d}M_i$ are the change in the ith eigenvalue, the change in the ith modal stiffness, and the change in the ith modal mass in the system.

On expanding and rearranging equation (14), we obtain

$$\frac{\mathrm{d}K_i}{K_i} = \frac{\mathrm{d}\lambda_i}{\lambda_i} + \frac{\mathrm{d}M_i}{M_i}\left(1 + \frac{\mathrm{d}\lambda_i}{\lambda_i}\right), \tag{15}$$

where $\mathrm{d}K_i/K_i$ represents the fractional change of the ith modal stiffness and all the terms on the right-hand side of the above equation can be determined directly or via experimental measurements.

For the ith mode and the jth location, the undamaged and damaged modal sensitivities, F_{ij} and F^*_{ij}, are related by the equation

$$F^*_{ij} = F_{ij} + \mathrm{d}F_{ij}, \tag{16}$$

where $\mathrm{d}F_{ij}$ represents the fractional change of modal energy at the jth member and for the ith mode. On differentiating equations (3) and (16), the quantity $\mathrm{d}F_{ij}$ can be obtained from

the expression

$$\mathrm{d}F_{ij} = \frac{K_{ij}}{K_i}\left[\frac{\mathrm{d}K_{ij}}{K_{ij}} - \frac{\mathrm{d}K_i}{K_i}\right], \tag{17}$$

where $\mathrm{d}K_{ij}$ represents the fractional change in K_{ij}. Also, by noticing $K_i \gg K_{ij}$, equation (17) can be reduced to the following form:

$$\mathrm{d}F_{ij} \cong \frac{\mathrm{d}K_{ij}}{K_i}. \tag{18}$$

Next, combining equations (2) and (6) and also combining equations (5) and (6), respectively, gives

$$K_{ij} = \gamma_{ij}E_j, \qquad K_{ij}^* = K_{ij} + \mathrm{d}K_{ij} = \gamma_{ij}^* E_j^*, \tag{19a, b}$$

in which $\gamma_{ij} = \Phi_i^{\mathrm{T}}\mathbf{C}_{j0}\Phi_i$ and $\gamma_{ij}^* = \Phi_i^{*\mathrm{T}}\mathbf{C}_{j0}\Phi_i^*$. Also from equation (19), $\mathrm{d}K_{ij}$ can be rewritten as

$$\mathrm{d}K_{ij} = \gamma_{ij}^*(E_j + \mathrm{d}E_j) - \gamma_{ij}E_j. \tag{20}$$

On dividing both sides of equation (20) by K_i (assuming $K_i \approx \gamma_i E_j$), substituting into equation (19), and only solving for the fractional change in the jth member's stiffness, we obtain

$$\frac{E_j}{E_j + \mathrm{d}E_j} = \left(\frac{\gamma_{ij}^*}{\gamma_i}\right) \Big/ \left(\frac{\mathrm{d}K_{ij}}{K_i} + \frac{\gamma_{ij}}{\gamma_i}\right). \tag{21}$$

Assuming the structure is damaged at a single location and the resulting change in K_{ij} is only the function of E_j, the first approximation of $\mathrm{d}K_{ij}$ can be obtained from the expression

$$\frac{\mathrm{d}K_{ij}}{K_i} = \left(\frac{\partial K_{ij}}{\partial E_j} + \frac{\partial K_{ij}}{\partial \gamma_{ij}}\frac{\partial \gamma_{ij}}{\partial E_j}\right)\frac{\mathrm{d}E_j}{K_i}, \tag{22}$$

in which

$$\partial K_{ij}/\partial E_j = \gamma_{ij}, \qquad \partial K_{ij}/\partial \gamma_{ij} = E_j, \tag{23a, b}$$

On substituting equation (23) into equation (22) and further approximating gives

$$\frac{\mathrm{d}K_{ij}}{K_i} \cong \frac{\gamma_{ij}}{\gamma_i}\frac{\mathrm{d}E_j}{E_j} + \frac{\mathrm{d}\gamma_{ij}}{\gamma_i} \tag{24}$$

and

$$\mathrm{d}\gamma_{ij} = \gamma_{ij}^* - \gamma_{ij}, \quad \gamma_i = \sum_{k=1}^{ne} \Phi_i^{\mathrm{T}}\mathbf{C}_{k0}\Phi_i. \tag{25}$$

Since we have assumed that the structure is damaged in a single location, it follows readily that $\mathrm{d}K_{ij} = \mathrm{d}K_i$ (note that $\mathrm{d}K_{ij} \approx \mathrm{d}K_i/nd$ if the structure is damaged in nd multiple

locations, in which the *nd* locations can be predicted). Then by substituting equation (15) into equation (24), the fractional changes in modal stiffness can be approximately related to the fractional changes in modal properties:

$$\frac{\mathrm{d}K_{ij}}{K_i} \cong g_i(\lambda, \Phi) = \frac{\mathrm{d}\lambda_i}{\lambda_i} + \frac{\mathrm{d}M_i}{M_i}\left(1 + \frac{\mathrm{d}\lambda_i}{\lambda_i}\right), \tag{26}$$

in which $g_i(\lambda, \Phi)$ is the dimensionless factor representing the systematic change in modal parameters of the ith mode due to the damage.

By applying equations (22)–(26) to equation (21), a new damage index for ith mode and jth location is given by

$$\beta_{ji} = \frac{E_j}{E_j^*} = \frac{\gamma_{ij}^*}{\gamma_i g_i(\lambda, \Phi) + \gamma_{ij}} = \frac{Num}{Den}. \tag{27}$$

For *nm* vibration modes, a damage index β_j for the jth location is obtained by

$$\beta_j = \sum_{i=1}^{nm} Num \Big/ \sum_{i=1}^{nm} Den. \tag{28}$$

Once damage is located at the jth member, damage severity of the jth member is estimated directly from equations (21), (27), and (28).

$$\alpha_j = \mathrm{d}E_j/E_j = 1/\beta_j - 1, \quad \alpha_j \geqslant -1, \tag{29}$$

where damage severity is indicated as the reduction in stiffness in the jth member if $\alpha_i < 0$.

The method described above yields information on the location and severity of damage directly from changes in mode shapes of structures. The appealing features of this method include the following: (1) damage can be located and sized using a few modes; (2) damage can be located and sized without solving a system of equations; and (3) damage can be located and sized in structures containing many members.

4. NUMERICAL VERIFICATION OF THE THEORY

The objective here is to evaluate the feasibility of the proposed algorithm to localize and estimate the severity of damage in a numerical model of a structure when only data on a few modes of vibration are available. We meet this objective in four steps: firstly, a test structure is defined and modal responses of the test structure are generated using the software package ABAQUS; secondly, a damage detection model of the test structure is selected; thirdly, the existing NDD algorithms (damage index A and damage index B) and the proposed algorithm (damage index C) are used to locate and estimate the severity of simulated damage in the test structure; and finally, the accuracy of NDD algorithm is evaluated by quantifying the damage prediction results. Here, by damage detection model we mean a mathematical representation of a structure with degrees of freedom corresponding to actual sensor readings or interpolated readings based on sensor readings at nearby locations.

4.1. DESCRIPTION OF TEST STRUCTURE

The test structure selected here is a theoretical model of a two-span continuous beam [16, 18]. In their previous work, Kim and Stubbs [16] identified a realistic theoretical model of a model plate-girder structure by fine-tuning experimental responses and a finite element model of the structure. As shown in Figure 1, the main structural subsystems of the theoretical model consisted of three element groups: (1) 50 beam members modelling the two-span continuous beam section; (2) two linear axial springs (Spring 1) modelling two outside supports; and (3) a linear axial spring (Spring 2) modelling a middle support. A typical arrangement of the test beam corresponding to 51 nodal points is schematized in Figure 1. In this hypothetical example we assume that only vertical motion is measured at each nodal point. Values for the material properties of the beam elements and springs were assigned as follows: (1) the elastic modulus $E = 70$ GPa; (2) Poisson's ratio $v = 0{\cdot}33$; and (3) the linear mass density $\rho = 2710\ \text{kg/m}^3$. Values for the geometric properties were assigned as follows: (1) for beam elements, the cross-sectional area $A = 1{\cdot}05 \times 10^{-3}\,\text{m}^2$ and the second moment of area $I = 7{\cdot}23 \times 10^{-7}\,\text{m}^4$; (2) for Spring 1 member, $A = 4{\cdot}96 \times 10^{-6}\,\text{m}^2$ and $I \approx 0$; and (3) for Spring 2 member, $A = 8{\cdot}4 \times 10^{-6}\,\text{m}^2$ and $I \approx 0$.

Next, we measured, via numerical simulation, the pre- and post-damage modal responses of the test structure. Here 10 damage cases are investigated, as summarized in Table 1. Each scenario represents a potential damage event that is typical to the existing beam-type bridges. It is also considered to account for the relationship between the modal sensitivity and the selected damage locations. A few locations that are relatively less sensitive to at least one mode are involved in the damage scenarios.

For example, Case 5 was selected to simulate an element near the middle support. Meanwhile, Case 7 was selected to simulate another element in the middle of the span. The first eight damage cases are limited to the model damaged only at a single location. Cases 6–8 focus on Element 39 in which three magnitude levels of damage are simulated. The last two damage cases (Cases 9 and 10) consider the model damaged in two locations. In all cases, damage was simulated in the structure by reducing the elastic modulus of the appropriate elements. Typical responses which are numerically generated (e.g., mode shapes and frequencies of the first three modes) are shown in Figure 2 and Table 1.

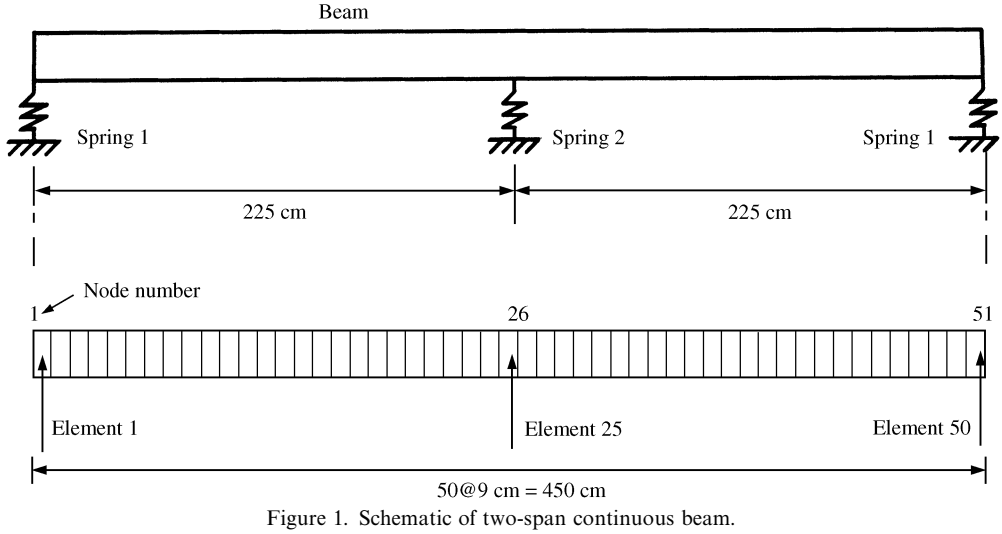

Figure 1. Schematic of two-span continuous beam.

TABLE 1

Damage scenarios and natural frequencies of two-span continuous beam

Damage case	Simulated damage		Natural frequency (Hz)		
	Location	Severity†	Mode 1	Mode 2	Mode 3
Undamaged	—	—	32·381	46·377	118·77
1	4	− 10	32·368	46·356	118·66
2	9	− 10	32·328	46·309	118·69
3	14	− 10	32·314	46·331	118·74
4	19	− 10	32·346	46·376	118·58
5	24	− 10	32·379	46·282	118·75
6	39	− 1	32·361	46·358	118·77
7	39	− 10	31·179	46·188	118·77
8	39	− 50	31·371	45·432	118·77
9	9, 34	− 10, − 10	32·276	46·297	118·52
10	14, 39	− 10, − 10	32·247	46·266	118·74

†Severity (%) $= (E^* - E)/E \times 100$.

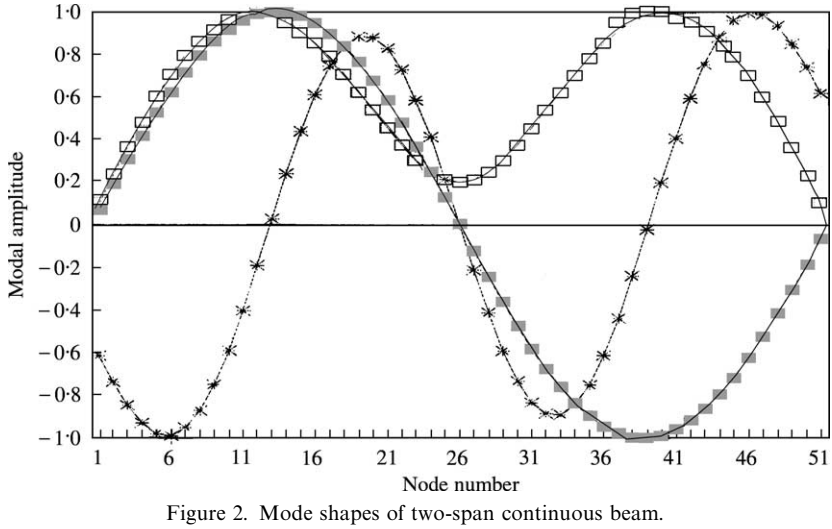

Figure 2. Mode shapes of two-span continuous beam.

4.2. DAMAGE LOCALIZATION AND SEVERITY ESTIMATION

Locations and severities of damage were predicted in the test structure. The two existing NDD algorithms (i.e., damage index A and damage index B) and the proposed NDD algorithm (i.e., damage index C) were examined. For each NDD algorithm involved, the damage localization and severity estimation are performed as follows. Firstly, pre- and post-damage modal parameters of the first three modes (as shown in Figure 2 and Table 1) were obtained from modal analysis of the test structure. Secondly, Euler–Bernoulli beam was selected as damage detection model of the test structure. This selection is based on the fact that the test model is a one-dimensional beam with only vertical motions are available.

From the mode shape of the ith modal vector $\phi_i(x)$, we generated a third order spline function, $w(x)$, for the beam using the 51 nodal displacements. Using the spline approximation of the mode shape, we computed the instantaneous curvature of the mode shape, $\phi_i''(x) = w''(x)$ at the 51 nodes of the test model. Then equivalent expressions for γ_{ij}, γ_{ij}^*, and γ_i in the damage index equations (e.g., equations (8), (12), and (27)) were computed by

$$\gamma_{ij} = \int_{x_k}^{x_k + \Delta x_k} \{\phi_i''(x)\}^2 \, \mathrm{d}x, \quad \gamma_{ij}^* = \int_{x_k}^{x_k + \Delta x_k} \{\phi_i''^*(x)\}^2 \, \mathrm{d}x, \quad \gamma_i = \int_0^L \{\phi_i''(x)\}^2 \, \mathrm{d}x, \tag{30}$$

in which x_k and $x_k + \Delta x_k$ correspond to two nodal locations of an element j for the beam model.

In Step 3, we established robust statistical criteria for damage localization. For a given set of modes, the locations of damage are selected on the basis of a rejection of hypotheses in the statistical sense [20, 21]. First, the value β_j ($j = 1, 2, 3, \ldots, ne$) associated with each member is treated as a random variable β. In other words, the collection of the damage indices β_j represents a sample population (we further assume the variables are distributed normally). The normalized indicator is given by

$$Z_j = (\beta_j - \bar{\beta}_i)/\sigma_i, \tag{31}$$

in which $\bar{\beta}_i$ and σ_i are mean and standard deviation of the collection of indicators of β_j values respectively. Next, the member is assigned to damage class via a statistical-pattern-recognition technique that utilizes hypothesis testing. The null hypothesis (i.e., H_0) is that the structure is not damaged at the jth location. The alternate hypothesis (i.e., H_1) is that the structure is damaged at the jth location. We define the decision rule as follows: (1) select H_0 (i.e., no damage exists at member j) if $Z_j < 2$ or (2) select the alternate H_1 if $Z_j \geqslant 2$. This criterion corresponds to a one-tailed test at a significance level of 0·023 (97·7% confidence level).

For damage index A, the damage indicator, equation (8), and the above criterion were used to select the potential damage location (see column 4 in Table 2). For damage index B, we repeated the exercises using equation (12) and the predicted potential damage locations (see column 6 in Table 2). Finally, for damage index C, we repeated the same procedures using equation (28) and the predicted potential damage locations (see column 8 in Table 2). Among the 10 damage cases, three cases were illustrated closely: damage case 1 (Figure 3), damage case 5 (Figure 4), and damage case 10 (Figure 5). Damage indices B and C have higher localization accuracy than damage index A (see also Table 2).

Finally, we estimated severities of damage at the predicted damage locations. Estimation was performed for damage indices A (i.e., equation (9)), damage index B (i.e., equation (13)), and damage index C (i.e., equation (29)) respectively. The severity estimation results are listed in Table 2 as follows: Column 5 for damage index A, Column 7 for damage index B, Column 9 for damage index C. Figures 3–5 show the accuracy of severity prediction for damage cases 1, 5, and 10 respectively. Damage index C shows the best results, while damage index A overestimated the severities and damage index B underestimated those values.

4.3. DAMAGE PREDICTION ACCURACY

The damage prediction accuracy was quantified by measuring metrical errors and by using the test of hypotheses as well [16, 22]. In this study, the uncertainty related to modelling errors, measurement errors, or any other types were not accounted in this

TABLE 2

Damage prediction results of two-span continuous beam

Damage case	Simulated damage		Predicted damage (damage index A)		Predicted damage (damage index B)		Predicted damage (damage index C)	
	Location	Severity†	Location	Severity†	Location	Severity†	Location	Severity†
1	4	− 10	1, 4 25, 26	− 12·8, − 18·9 − 8·6, − 23·5	4	− 3·8	4	− 11·9
2	9	− 10	1, 9 26	− 11·6, − 18·7 − 20·9	9	− 1·3	9	− 10·7
3	14	− 10	14, 26	− 18·3, − 31·4	14	− 1·4	14	− 9·4
4	19	− 10	19, 26	− 18·1, − 16·8	19	− 0·8	19	− 9·5
5	24	− 10	24, 25 26	− 15·7, − 18·7 − 7·6	24	− 0·5	24	− 9·3
6	39	− 1	25, 26 (−), 49	− 11·1, − 7·3 (−), − 5·2	39	− 0·1	39	− 1·0
7	39	− 10	25, 39	− 29·0, − 18·5	39	− 1·5	39	− 9·6
8	39	− 50	25, 39	− 6·72, − 72·7	39	− 14·8	39	− 46·4
9	9, 34	− 10, − 10	9, 34 50	− 18·3, − 17·5 − 7·7	9, 34	− 1·3, − 1·1	9, 34	− 11·1, − 8·0
10	14, 39	− 10, − 10	14, 26 39	− 17·4, − 11·3 − 17·7	14, 39	− 1·4, − 1·4	14, 39	− 10·3, − 10·9

† Severity (%) $= (E^* - E)/E \times 100$.

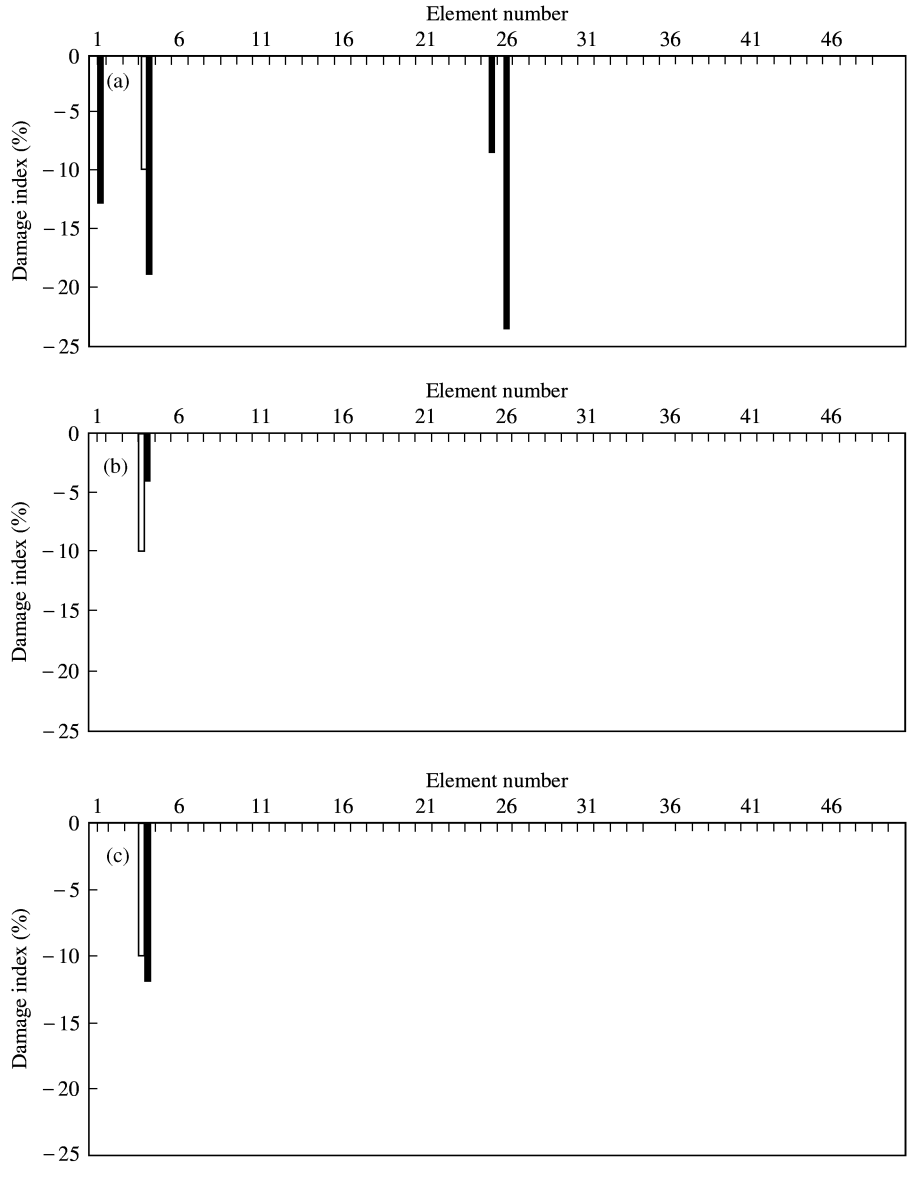

Figure 3. Damage prediction results of damage case 1. (a) Damage Index A, (b) Damage Index B, (c) Damage Index C. □, True; ■ Predict.

accuracy assessment. As the first NDD accuracy measure, we selected a mean localization error (*mle*) defined as

$$mle = \frac{1}{N} \sum_{i=1}^{N} |x_i^t - x_i^p| / L, \quad 0 \leqslant mle \leqslant 1, \tag{32}$$

where N is the number of damage cases, x_i^t and x_i^p are the true location and the predicted location of the ith damage case, respectively, and L is a characteristic distance (e.g., a span of the beam model).

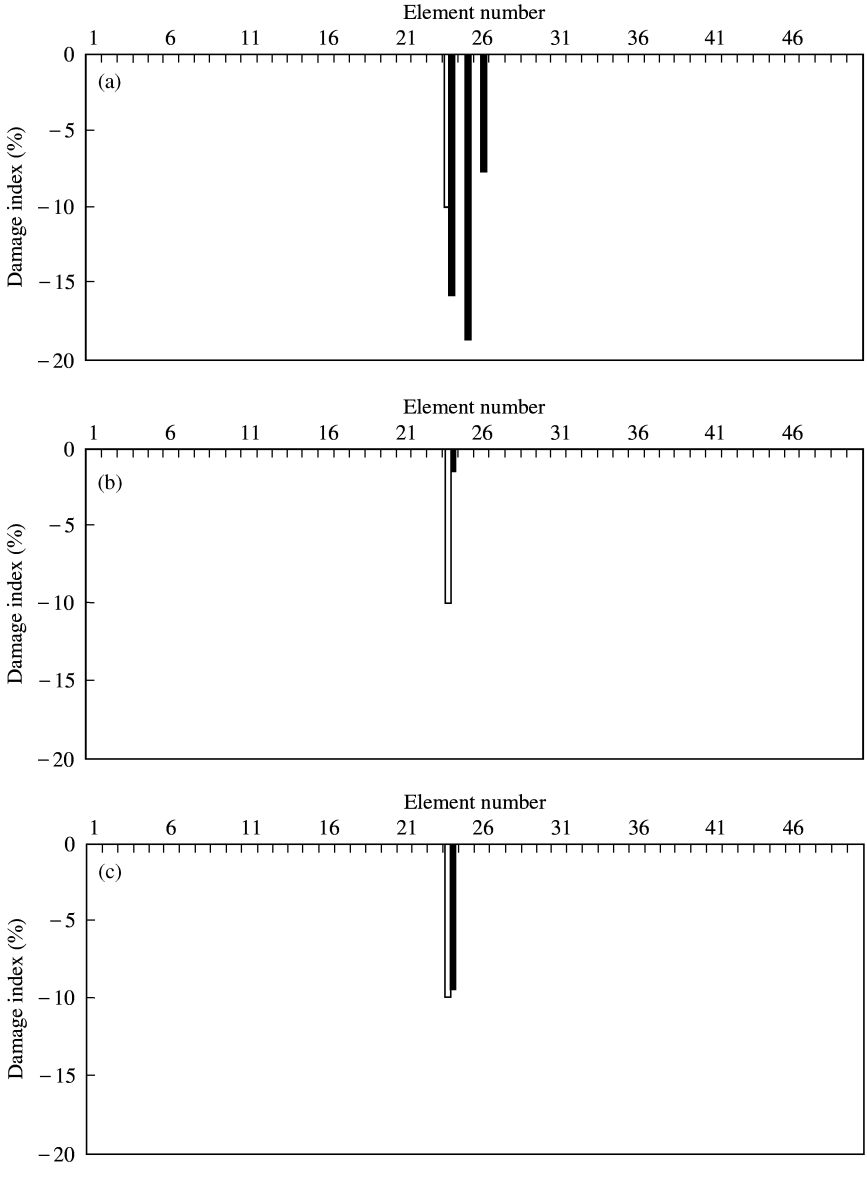

Figure 4. Damage prediction results of damage case 5.(a) Damage Index A, (b) Damage Index B, (c) Damage Index C. □, True; ■ Predict.

As the second NDD accuracy measure, we selected a detection missing error (*dme*) defined as

$$dme = \frac{1}{NT} \sum_{i=1}^{N} TI, \quad 0 \leqslant dme \leqslant 1, \tag{33}$$

where NT is the number of true damage locations, TI is the number of Type I errors (fail in detection of true damage locations) for the number of true damage locations. The *dme* measures false negative errors such that true damage locations are not predicted. If $dme = 0$, it means that all true damage locations are predicted.

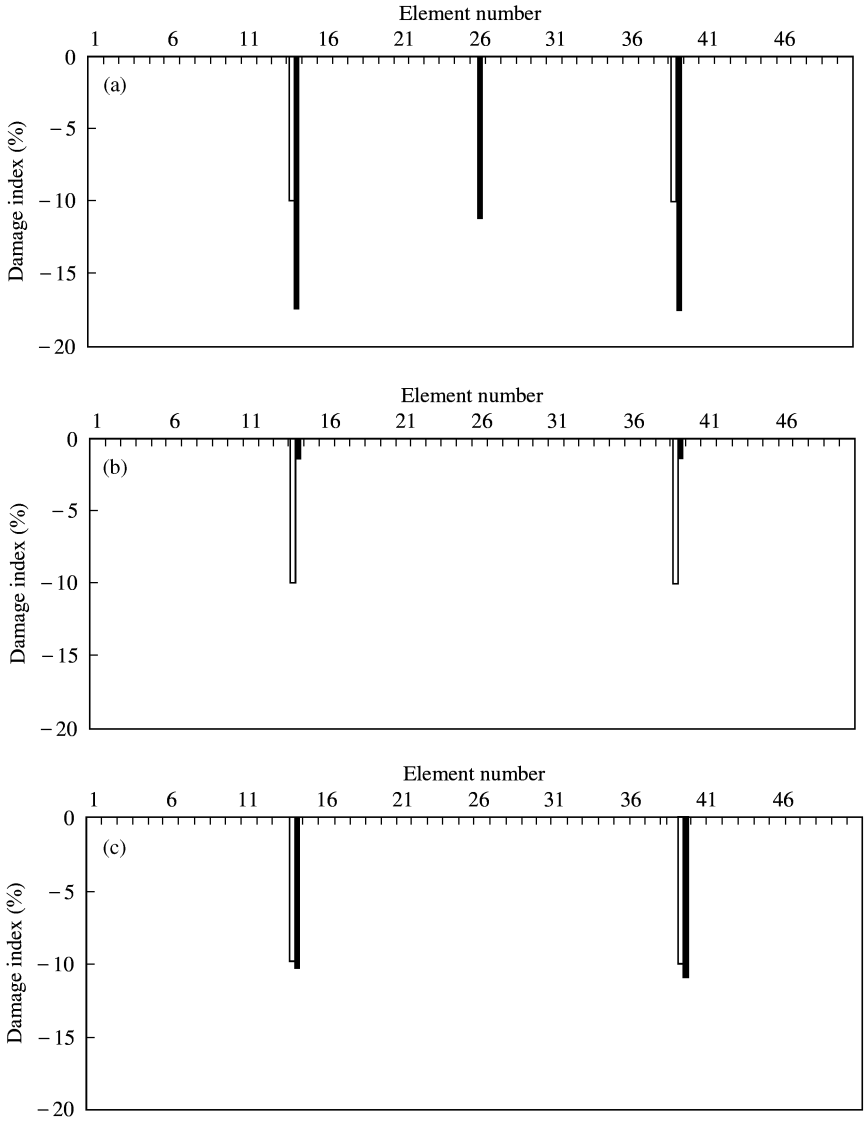

Figure 5. Damage prediction results of damage case 10. (a) Damage Index A, (b) Damage Index B, (c) Damage Index C. □, True; ■ Predict.

As the third NDD accuracy measure, we selected a false alarm error (*fae*) defined as

$$fae = \frac{1}{NF} \sum_{i=1}^{N} TII, \quad 0 \leqslant fae < \infty, \tag{34}$$

where NF is the number of the predicted locations, TII is the number of Type II errors (prediction of locations that are not damaged). The *fae* measures false-positive errors such that predicted locations are not the true damage locations. If $fae = 0$, then all predicted locations correctly locate the damage.

As the last NDD accuracy measure, we selected a mean sizing error (*mse*) that is defined as

$$mse = \frac{1}{NF} \sum_{i=1}^{N} |(\alpha_i^t - \alpha_i^p)/\alpha_i^p|, \quad 0 \leqslant mse \leqslant \infty, \tag{35}$$

where α_i^t and α_i^p are, respectively, a true damage severity and a predicted damage severity for ith location. The *mse* measures the NDD algorithm's accuracy in severity estimation and the value close to zero means that the severity estimation error is close to zero.

We implemented the four NDD accuracy measures given by equations (32)–(35) to the damage localization and severity estimation results of each NDD algorithm. Then the accuracy of each NDD algorithm was quantified as listed in Table 3. From the table, three major results are observed. Firstly, the accuracy measures for damaged index A are analyzed as follows: (1) a *dme* of 0·083 indicates that 11 out of 12 true damage locations can be predicted; (2) a *fae* of 0·57 indicates that about 6 out of 10 predicted locations can be false-positive (i.e., about 60% of predicted locations are false-alarmed); (3) a *mle* of 0·133 indicates that damage can be located within about a distance of $0{\cdot}13L$ (13% of span length) from the correct location of damage; and (4) a *mse* of 0·75 indicates that the estimated severities show an average 75% error and it consistently overestimates severity levels by about 1·75 times of the true damage sizes.

Secondly, for damage index B, the accuracy measures are interpreted as follows: (1) all localization error measures (*dme*, *fae*, and *mle*) are zero (i.e., there are no localization errors) and (2) a *mse* of 0·853 indicates that the estimated severities show an average 85·3% error and it consistently underestimates severity levels by about 0·15 times of the true damage sizes. Finally, for damage index C, the accuracy measures are interpreted as follows: (1) all localization error measures are zero (i.e., there are no localization errors) and (2) a *mse* of 0·077 indicates that the estimated severities show an average 7·7% error. As listed in Table 2, the predicted severities are very close to the true damage sizes. Compared to two other NDD algorithms, damage index C enhanced the accuracy of the damage localization and severity estimation results.

In a previous study [16], the impact of the uncertainty in mode shapes measurements on the accuracy of damage localization using damage index B was studied. Mode shape measurements were assigned uncertainties associated with coefficients of variation (COV) ranging from 0·01 to 0·3. As expected, the uncertainty in mode shape measurements did influence such performance indicators of the damage detection scheme as the number of Type I errors, the number of Type II errors, and the error in the predicted magnitude of the damage. However, for the worst case ($COV = 0{\cdot}3$), it was concluded that damage could be confidently located to within a fraction of 0·13 the length of the span and the error in the

TABLE 3

Quantification of damage prediction accuracy

Damage detection algorithm type	Measures of damage prediction accuracy			
	dme	*fae*	*mle*	*mse*
Damage index A	0·083	0·570	0·133	0·750
Damage index B	0	0	0	0·853
Damage index C	0	0	0	0·077

severity estimation was less than 24% [16]. Although the existing algorithms show their robustness in the uncertainty circumstances, the relative impact of the uncertainties on the accuracy of damage identification using damage index C will be examined as an extended study.

5. SUMMARY AND CONCLUSIONS

The objective of this paper was to present an improved, vibration-based, damage detection algorithm which was newly derived and to evaluate the accuracy of the algorithm when applied to a two-span continuous beam. This objective was achieved in two parts. In this first part, we reviewed existing damage detection algorithms and their limits in the accuracy of damage detection. Then we formulated a new damage detection algorithm that overcomes the limits of the existing algorithms and improved its accuracy in damage localization and severity estimation. In the second part, two existing algorithms and the new algorithm were evaluated by predicting damage location and severity estimation in a theoretical model of a two-span continuous beam. Each algorithm was assessed quantifying the accuracy of damage localization and severity estimation results.

By applying the approach to the numerical example, we obtained the following relationships between the algorithms and their accuracy in damage prediction. First, the use of damage index A for the damage prediction exercises resulted in (1) relatively small Type I error (false detection of true damage locations); (2) small localization error; (3) relatively high Type II error (prediction of locations that are not damaged); and (4) high severity estimation error. It consistently overestimated severities of damage by about 1·75 times of the true damage sizes. Second, the use of damage index B resulted in no error related to damage localization but high severity estimation error. It consistently underestimated severities by about 0·15 times of the true damage sizes. Finally, the use of damage index C resulted in no error related to damage localization and very small severity estimation error. Compared to two other algorithms, damage index C enhanced the accuracy of the damage localization and severity estimation results.

ACKNOWLEDGMENT

The funding for the study was provided by Korea Institute of Construction Technology. The authors would like to extend their thanks to KICT for the support.

REFERENCES

1. E. KUMMER, J. C. S. YANG and N. G. DAGALAKIS 1981 *2nd American Society of Civil Engineering/EMD Specialty Conference, Atlanta, Georgia*, 445–460. Detection of fatigue cracks in structural members.
2. J. C. S. YANG, J. CHEN and N. G. DAGALAKIS 1984 *Journal of Energy Resources Technology. American Society of Mechanical Engineers* **106**, 38–42. Damage detection in offshore structures by the random decrement technique.
3. R. G. FLESCH and K. KERNICHLER 1988 in *Workshop on Structural Safety Evaluation Based on System Identification Approaches* (H. G. Natke and J. T. P. Yao, editors), 433–459, Lambrecht/ Pfalz, Germany: Vieweg & Sons. Bridge inspection by dynamic tests and calculations dynamic investigations of Lavent bridge.
4. S. F. MASRI, R. K. MILLER, A. F. SAUD and T. K. CAUGHEY 1987 *Journal of Applied Mechanics* **54**, 923–929. Identification of nonlinear vibrating structures: Part I—formulation.

5. H. G. NATKE and J. T. P. YAO 1990 *International Conference on Structural Safety and Reliability*, *American Society of Civil Engineers*, *New York*, 1387–1393. System identification methods for fault detection and diagnosis.
6. P. GUDMUNSON 1982 *Journal of Mechanics and Physics of Solids* **30**, 339–353. Eigenfrequency changes of structures due to cracks, notches or other geometrical changes.
7. P. GUDMUNSON 1983 *Journal of Mechanics and Physics of Solids* **31**, 329–345. The dynamic behavior of slender structures with cross-sectional cracks.
8. S. CRISTIDES and A. D. S. BARRS 1984 *International Journal of Mechanical Science* **26**, 639–648. One-dimensional theory of cracked Bernoulli–Euler beams.
9. R. D. ADAMS, P. CAWLEY, C. J. PYE and B. J. STONE 1978 *Journal of Mechanical Engineering Science* **20**, 93–100. A vibration techniques for non-destructively assessing the integrity of structures.
10. P. CAWLEY and R. D. ADAMS 1979 *Journal of Strain Analysis* **14**, 49–57. The location of defects in structures from measurements of natural frequencies.
11. T. K. O'BRIEN 1980 in *Mechanics of Non-destructive Testing* (W. W. Stinchcomb, editor), 101–121. New York: Plenum Press. Stiffness change as a nondestructive damage measurement.
12. R. M. KENLEY and C. J. DODDS 1980 *Offshore Technical Conference*, *Houston*, *Texas*, 111–118. West sole WE platform: detection of damage by structural response measurements.
13. M. BISWAS, A. K. PANDEY and M. M. SAMMAN 1990 *NATO Advanced Research Workshop on Bridge Evaluation*, *Repair and Rehabilitation* (A. Noward, editor), 161–174. Maryland: Kluwer Academic Publishers. Modal technology for damage detection of bridges.
14. N. STUBBS and R. OSEGUEDA 1990 *International Journal of Analytical and Experimental Modal Analysis* **5**, 67–79. Global non-destructive damage evaluation in solids.
15. J. CHEN and J. A. GARBA 1988 *American Institute of Aeronautics and Astronautics Journal* **26**, 1119–1126. On-orbit damage assessment for large space structures.
16. J. T. KIM and N. STUBBS 1995 *Journal of Structural Engineering*, *American Society of Civil Engineers* **121**, 1409–1417. Model-uncertainty impact and damage-detection accuracy in plate girder.
17. A. E. AKTAN, K. L. LEE, C. CHUNTAVAN and T. AKSEL 1994 *Proceedings of the* 12*th International Modal Analysis Conference*, Vol. 1, 462–468. Model testing for structural identification and condition assessment of constructed facilities.
18. N. STUBBS and J. T. KIM 1996 *American Institute of Aeronautics and Astronautics Journal* **34**, 1644–1649. Damage localization in structures without baseline odal parameters.
19. C. R. FARRAR and D. A. JAUREGUI 1998 *Smart Materials and Structures* **7**, 704–719. Comparative study of damage identification algorithm applied to a bridge: I. Experiment.
20. K. FUKUNAGA 1990 *Introduction to Statistical Pattern Recognition.* New York: Academic Press.
21. J. D. GIBSON and J. L. MELSA 1975 *Introduction to Nonparametric Detection with Applications.* New York: Academic Press.
22. B. KOSKO 1992 *Neural Networks for Signal Processing*. Englewood Cliffs, NJ: Prentice-Hall.